AMERICAN MUSEUM NOVITATES

Number 3922, 25 pp. March 4, 2019

Intraspecific variation through ontogeny in Late Cretaceous ammonites

CARINA KLEIN[1] AND NEIL H. LANDMAN[2]

ABSTRACT

This project assesses intraspecific variation through the ontogeny of the ammonite *Scaphites whitfieldi* Cobban, 1951, from the Upper Cretaceous of the U.S. Western Interior. Our sample consists of 103 dorsoventral cross sections from nine localities that represent two lithofacies (shale and siltstone). We measured four shell parameters (ww/dm, ww/wh, uw/dm, and WER) to describe the ontogenetic changes in shell morphology. We investigated the variation at three growth stages: immediately after hatching (dm = 1 mm), the neanoconch (dm = 4 mm), and the submature stage (defined as at or near the base of the mature hooklike body chamber). In general, the shell becomes more discoidal through ontogeny with a narrower umbilicus and a more compressed whorl section. The results of the univariate analysis indicate that the variation is statistically significantly higher in the neanoconch than in either the hatchling or submature stage. This pattern is also apparent in the multivariate analysis in which the disparity increases markedly from the hatchling to the neanoconch and then decreases again at the submature stage. These results are consistent with the hypothesis that the neanoconch represents a transition in the life history of the animal to a more demersal mode of life followed by a canalization of morphology toward maturity. However, because the neanic transition occurs over a range of sizes, it is possible that some individuals may have already undergone these changes at dm = 4 mm, whereas others may not have, thus inflating the degree of variation. To resolve this issue in the future, it is critical to examine each ontogenetic trajectory individually to pinpoint the exact size at which the morphological changes occur. We also compared the values of ww/dm, ww/wh, uw/dm, and WER of the three growth stages for the sample from siltstone versus the sample from shale. The comparison reveals that the specimens from siltstone occupy lower regions of the morphospace,

[1] Museum für Naturkunde, Berlin.
[2] Division of Paleontology (Invertebrates), American Museum of Natural History, New York.

 ISSN 0003-0082

implying that these specimens are generally more compressed than those from shale. This difference may be related to selection pressures for improved hydrodynamic efficiency in the higher energy environment represented by siltstone.

INTRODUCTION

Ammonites provide a rare opportunity to investigate the complete record of the ontogenetic development of an individual based on a single shell. Because the growth of the shell is accretionary, it is possible to examine all the successive ontogenetic stages by carefully breaking down or sectioning adults. This advantage has been one of the mainstays of ammonite studies for the past 150 years. Starting with the pioneering work of Branco (1879–1880) and Hyatt (1893), who documented the embryonic shells of ammonites, to Schindewolf (1954), who traced the ontogenetic development of suture lines, to Druschits and Doguzhaeva (1981), who illustrated the ontogenetic development of shell microstructure, this line of inquiry has powered major investigations in ammonite research. As enunciated by Hyatt (1894: 351): "How unreasonable it would seem to a student of fossil Mammalia, if he were requested to do what it would be appropriate to require from a student of the fossil Cephalopoda … to describe from the investigation of a single perfect fossil skeleton of an adult, not only the characteristics of the skeleton at the stage of growth at which the animal died, but [all] the development stages…."

The accretionary growth of the ammonite shell also accounts for the popularity of these fossils in countless studies of recapitulation and heterochrony, especially as an example of what Wiedmann and Kullmann (1980: 215) called "additive typogenesis," one of the guiding principles in working out the phylogenetic sequence of sutures (for a review of such studies, see Landman, 1988). The capability of reconstructing the complete ontogeny of an ammonite from a single specimen also underscores the relevance of these fossils to present-day studies of evo-devo where small changes in development can lead to big changes in evolution. This approach also facilitates inquiries into the constructional constraints that underlie the ontogenetic expression of morphology, as formulated, for example, in Buckman's Law of Covariation (Yacobucci, 2004; Landman et al., 2017: 117–120).

To obtain data about ammonite ontogenetic development, the shape of the shell (or at least an approximation of it) can be captured by measuring the diameter, whorl width, whorl height, and umbilical width through ontogeny. Raup (1967), building on the previous work of Moseley (1838) and Thompson (1917), derived several simple ratios and equations to express the shape of the shell and its expansion rate, which form the basis of all modern methods for describing ammonite morphospace (Korn, 2012). Using whole specimens or dorsoventral and median cross sections, one can accurately describe the morphological changes through ontogeny. These ratios can in turn be used to determine the length of the living chamber, the positions of the centers of mass and buoyancy, and the orientation of the aperture in the water column, all of which affect the hydrostatic and hydrodynamic properties of the shell (Jacobs and Chamberlain, 1996; Korn and Klug, 2012).

In this study, we are interested in questions of intraspecific variation through ontogeny. Many patterns of ontogenetic variation have been described in ammonites. Some studies have

argued that the highest variation appears in early ontogeny (Tanabe and Shigeta, 1987; Monnet et al., 2012; for modern *Nautilus*, see Tajika et al., 2018), while others have suggested that the highest variation occurs in middle ontogeny (Dagys and Weitschat, 1993; Korn and Klug, 2007; De Baets et al., 2013), and still others have suggested that the highest variation occurs at the end of ontogeny in the form of sexual dimorphism (Klug et al., 2015). We approach this subject by examining the intraspecific variation at three stages in the ontogeny of a single species of Late Cretaceous ammonite. We ask the following questions: How does morphological variation plot against ontogenetic development? Is the degree of variation higher at one ontogenetic stage than another? Does variation expand or contract during ontogeny? How does the degree of variation at each ontogenetic stage correlate with environmental factors (facies)? Does the degree of variation at each stage differ between samples from the same site (derived from single versus multiple concretions)? Does the variation at each stage differ between sexual dimorphs of the same species? These questions are fundamental to our understanding of ontogenetic development and, inasmuch as variation is the raw material for natural selection, these questions also bear on the process of evolution.

MATERIAL

We focus on a single ammonite species *Scaphites whitfieldi* Cobban, 1951, from the upper Turonian (Upper Cretaceous) of the U.S. Western Interior (figs. 1, 2). This species was assigned to the new genus *Coloradoscaphites* by Cooper (1994). However, this assignment has not been followed by any subsequent worker and, until a thorough phylogenetic revision of all the Turonian-Santonian scaphites of the U.S. Western Interior is undertaken, we prefer to follow the simplified taxonomy outlined in Cobban et al. (2006). Maturity in this species, as in other scaphites, is expressed by the uncoiling of the final body chamber, permitting a clear delimitation of variation at this stage of growth. *Scaphites whitfieldi* exhibits a broad geographic distribution extending from Canada to New Mexico and from Utah to Colorado. It occurs in two facies, siltstone and shale, permitting an investigation of intraspecific variation with respect to the environment (fig. 3). In addition, this species is confined to a single ammonite biozone (Cobban et al., 2006), so that the samples, although broad ranging, are approximately time-equivalent within the limits of resolution afforded by biostratigraphy. Furthermore, because many specimens are preserved in early diagenetic concretions, they retain their original three-dimensional shape, making them ideal for morphometric analysis (for a discussion about the origin of early diagenetic concretions, see Landman and Klofak, 2012). Specimens of this species are also abundant, furnishing large sample sizes for analysis. For example, Landman (1987) reported 113 specimens in a single concretion from the Turner Sandy Member of the Carlile Shale of Wyoming.

We examined 103 adults of *Scaphites whitfieldi*. Adults of this species range from 23 to 53 mm in maximum length (Landman, 1987: fig. 77). They are quadrangular in side view and are covered with dense, evenly spaced ribs (fig. 1). The exposed phragmocone is closely coiled and occupies approximately one whorl, generally ending below the line of maximum length. The

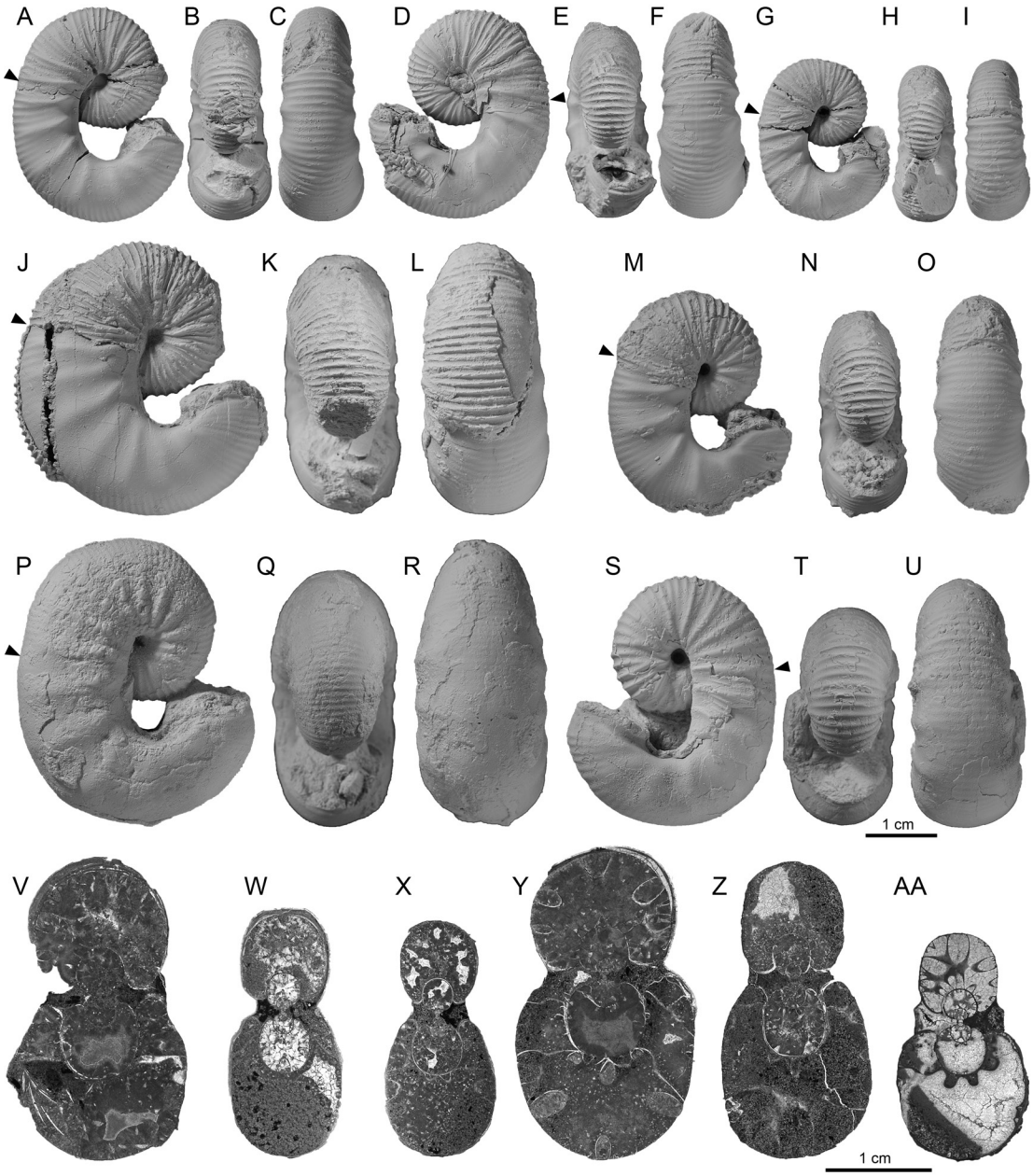
A
B
C
D
E
F
G
H
I
J
K
L
M
N
O
P
Q
R
S
T
U
1 cm
V
W
X
Y
Z
AA
1 cm

body chamber consists of a shaft and recurved hook terminating in a constricted aperture. The umbilical shoulder of the shaft is straight in side view. The uncoiling of the body chamber creates a large gap between the phragmocone and aperture.

Dimorphism is present in *Scaphites whitfieldi*, but the morphological differences between dimorphs are not as well expressed as in more advanced genera of scaphites such as *Hoploscaphites* (for a discussion of dimorphism in scaphites, see Landman and Waage, 1993; Landman et al., 2010). In *S. whitfieldi*, adult macroconchs (females?) are larger, more robust, and more involute than adult microconchs (males?). Specimens at the extreme ends of the size spectrum are easily assigned to their respective dimorphs (compare figs. 1J–L and M–O). However, most adults of this species fall in a transitional size range, and it is difficult to assign them to their respective dimorphs (fig. 1S–U). As Landman (1987: 217) stated, "the dimorphs themselves are intergradational in shape over this size range and the morphological criteria previously used to discriminate dimorphs are ineffective at these sizes." Therefore, in our study, we did not distinguish between dimorphs except in a single small sample.

The specimens in our study are from nine localities spanning approximately 1300 km north-south and 1000 km west-east (table 1, fig. 3, appendix 2). The study localities are (from north to south): (1) the Ferdig Shale Member of the Marias River Shale, Toole County, Montana (B240), (2) the Turner Sandy Member of the Carlile Shale, Butte County, South Dakota (B185-187, B198), (3) the Turner Sandy Member of the Carlile Shale, Fall River County, South Dakota (B192), 4) the Turner Sandy Member of the Carlile Shale, Niobrara County, Wyoming (B176), (4) the Juana Lopez Member of the Mancos Shale, Routt County, Colorado (D9111), and (5) the Ferron Sandstone Member of the Mancos Shale, Emery County, Utah (D7227). These localities represent two facies (shale and siltstone) based on the facies map of McGookey et al. (1972). The "shale" consists of mud and silt and the "siltstone" consists of silt and fine-grained sand. Localities B185–187, B198, B240, and D9111 represent shale and B176, B192, and D7227 represent siltstone (fig. 3).

FIGURE 1. *Scaphites whitfieldi* Cobban, 1951, adults. **A–I.** USGS Mesozoic loc. D7227, Ferron Sandstone Member, Mancos Shale, Emery County, Utah. **A–C.** AMNH 82701, microconch, right, apertural, and ventral views. **D–F.** AMNH 82700, microconch, right, apertural, and ventral views. **G–I.** AMNH 82702, microconch, right, apertural, and ventral views. **J–O.** USGS Mesozoic loc. D9111, Juana Lopez Member, Mancos Shale, Routt County, Colorado. **J–L.** AMNH 82698, macroconch, right, apertural, and ventral views. **M–O.** AMNH 82697, microconch, right, apertural, and ventral views. **P–U.** B192s, Turner Sandy Member, Carlile Shale, Fall River County, South Dakota. **P–R.** AMNH 82696, macroconch (?), right, apertural, and ventral views. **S–U.** AMNH 82694, microconch (?), right, apertural, and ventral views. V–AA. Dorsoventral sections. **V.** YPM 391061, B176, Turner Sandy Member, Carlile Shale, Niobrara County, Wyoming. **W.** YPM 391008, B176a, single concretion, Turner Sandy Member, Carlile Shale, Niobrara County, Wyoming. **X.** YPM 390993, B176a, single concretion, Turner Sandy Member, Carlile Shale, Niobrara County, Wyoming. **Y.** YPM 391066, B176, Turner Sandy Member, Carlile Shale, Niobrara County, Wyoming. **Z.** YPM 391157, B192, Turner Sandy Member, Carlile Shale, Fall River County, South Dakota. **AA.** AMNH 82704, B187, Turner Sandy Member, Carlile Shale, Butte County, South Dakota. Arrows indicate the base of the mature body chamber.

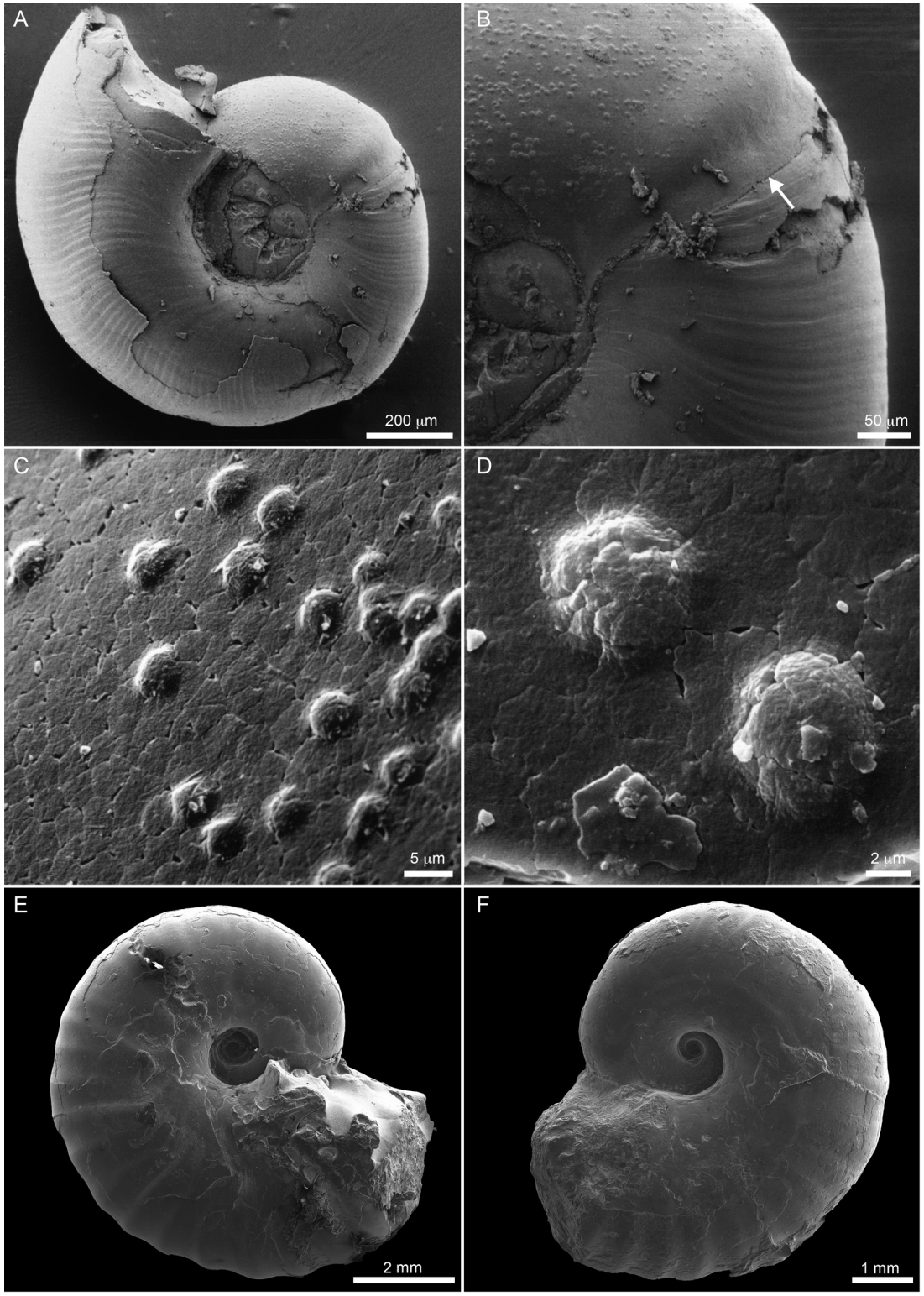
A
200 μm
B
50 μm
C
5 μm
D
2 μm
E
2 mm
F
1 mm

TABLE 1. Localities, number of specimens, county, state, and facies of *Scaphites whitfieldi* used in this study, listed according to facies. Abbreviations: prefix B = Yale Peabody Museum locality; D = U.S. Geological Survey locality; AMNH = AMNH locality; B176a and B192s = single concretions (see appendix 2 for detailed information).

Locality	Number of specimens	County, State	Facies
B185-187, 198	12 (2, 3, 3, 4, respectively)	Butte Co., SD	Shale
B240	12	Toole Co., MT	Shale
D9111	16	Routt Co., CO	Shale
B176a, 176	28 (12, 16, respectively)	Niobrara Co., WY	Siltstone
B192s, B192 = AMNH 3421	23 (8, 15, respectively)	Fall River Co., SD	Siltstone
D7227	12	Emery Co., UT	Siltstone

METHODS

The ontogenetic development of *Scaphites whitfieldi* was studied by examining adults, that is, individuals that survived to maturity. We prepared dorsoventral cross sections in which the plane of the section contains the axis of coiling and passes through the protoconch and at or near the base of the adult body chamber (fig. 1V–AA) (for an overview about grinding techniques used in ammonites; see Naglik et al., 2015; for a discussion about the comparative merits of median and dorsoventral cross sections, see Landman, 1987: 163–169). The cross sections were carefully prepared to avoid introducing artifacts, as noted by Kant and Kullmann (1973). The cross sections are archived at the American Museum of Natural History (AMNH), New York, and the Yale Peabody Museum (YPM), New Haven, Connecticut. In three specimens, the preservation at the base of the body chamber was poor, and so this ontogenetic stage was not included in the analysis of these three specimens.

Using digitized drawings of the cross sections, we measured whorl width, whorl height, and umbilical width, starting at the beginning of ontogeny, and calculated four ratios (ww/wh, ww/dm, uw/dm, and WER), as illustrated in figure 4. The ratio ww/dm has been called the "thickness ratio" in studies describing the hydrodynamic properties of ammonite shells (Jacobs and Chamberlain, 1996). These ratios are plotted against log diameter, following standard procedures (Korn, 2012), beginning at dm = 1 mm, to yield ontogenetic trajectories.

To determine intraspecific variation through ontogeny, we chose to examine three ontogenetic stages:

1. Hatchling (fig. 2A–D). The embryonic shell (ammonitella) probably formed inside an egg capsule (Landman and Waage, 1982). In scaphites, the ammonitella is covered with

FIGURE 2. *Scaphites whitfieldi* Cobban, 1951, hatchlings and neanoconchs. **A–D.** AMNH 44833, B198, Turner Sandy Member, Carlile Shale, Butte County, South Dakota. **A.** Newly hatched shell consisting of the ammonitella and part of the succeeding whorl. **B.** Close-up of the primary constriction and ammonitella edge (arrow). **C, D.** Close-ups of tubercles on the lateral side of the ammonitella. **E.** Neanoconch plus part of the succeeding whorl, AMNH 82693, dm = 7.3 mm, right lateral, USGS Mesozoic loc. D7227, Ferron Sandstone Member, Mancos Shale, Emery County, Utah. **F.** Neanoconch plus part of the succeeding whorl, AMNH 82692, dm = 6.3 mm, left lateral, B198a, Turner Sandy Member, Carlile Shale, Butte County, South Dakota.

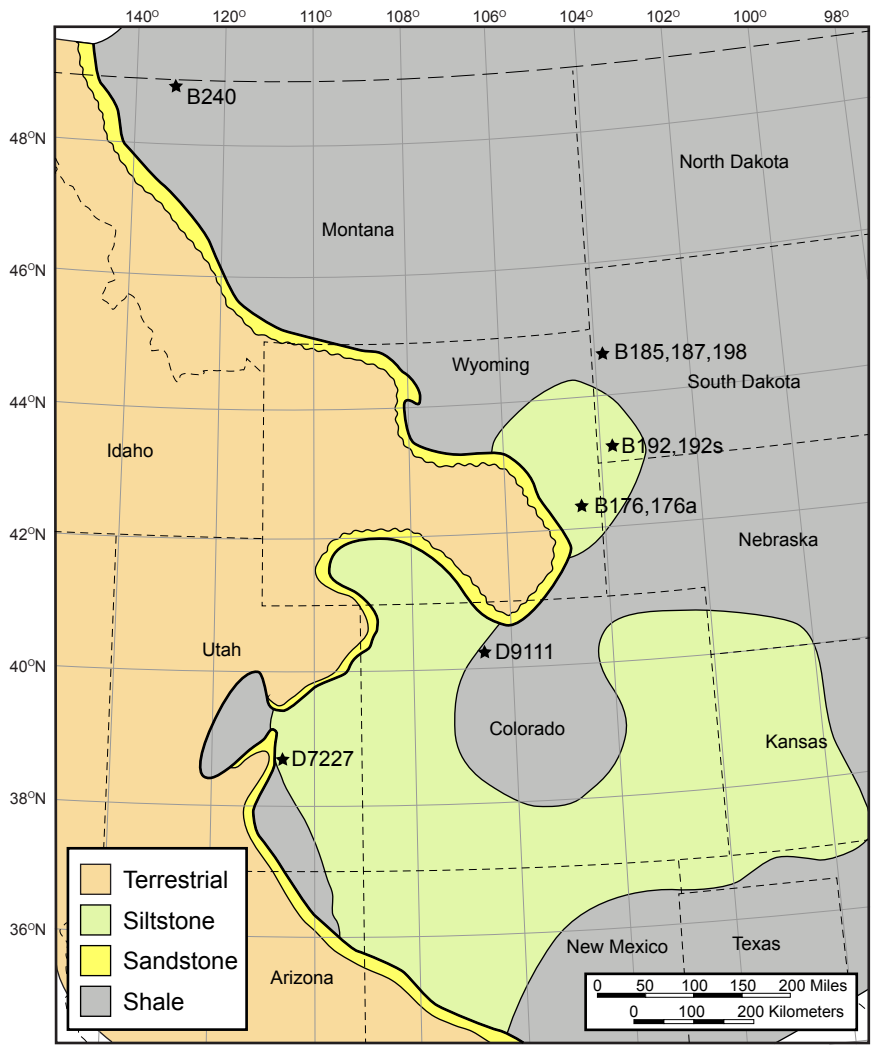

FIGURE 3. Facies map of the Western Interior Seaway during the deposition of the lower Turonian *Scaphites whitfieldi* Zone (simplified from McGookey, 1972). The localities are indicated by stars.

a tuberculate microornamentation, which disappears at the end of the primary constriction (Landman et al., 1996). The newly hatched ammonite may have spent several weeks to months in the plankton (Landman et al., 2012a). In *Scaphites whitfieldi*, the diameter of the ammonitella averages 619 um (n = 198, Landman, 1987). In order to compare the morphology of the newly hatched shell, we targeted a diameter of 1 mm, comprising the ammonitella and part of the succeeding whorl. We obtained the values for the four ratios at this diameter by interpolation, using the plots of the ratios versus log diameter.

2. Neanoconch (fig. 2E, F). The first postembryonic stage is called the neanic stage and the animal or shell that formed during this stage is called the neanoconch. It consists of approximately two whorls beyond the end of the ammonitella, corre-

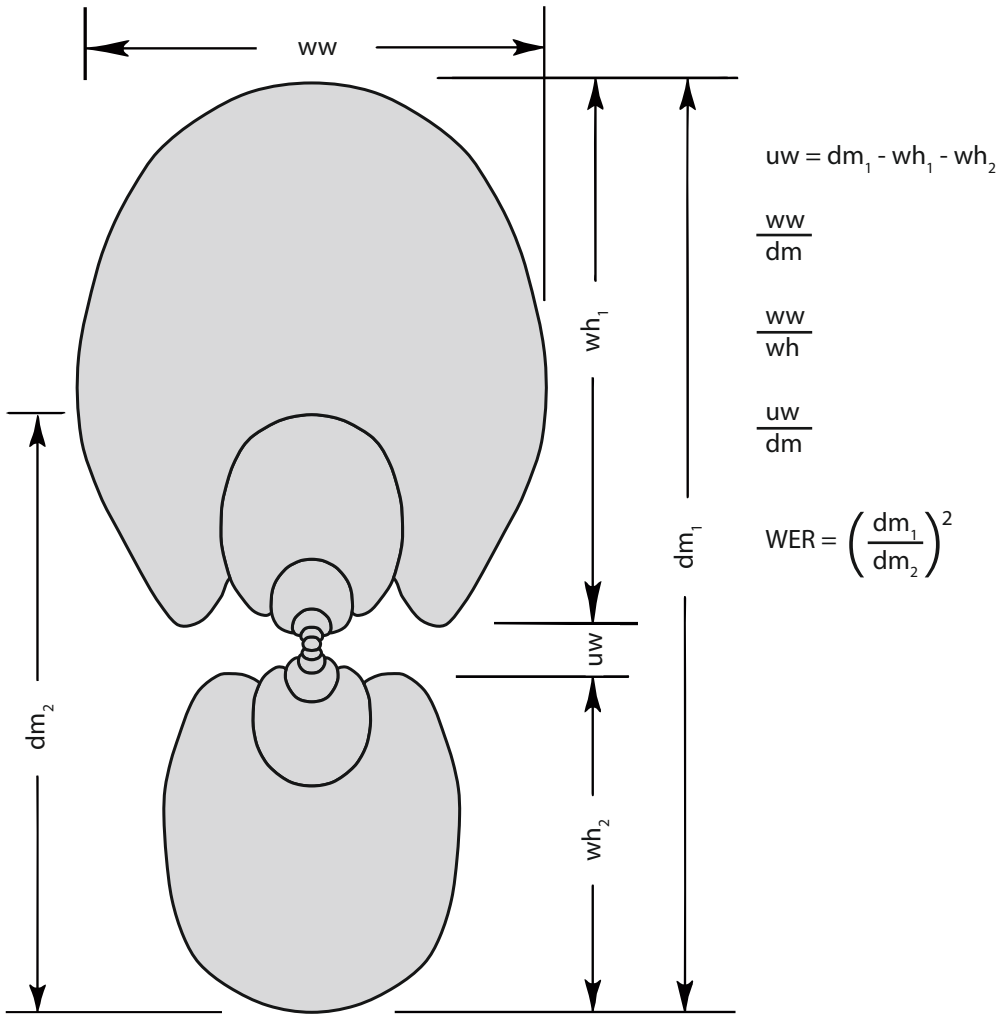

FIGURE 4. Measurements of *Scaphites whitfieldi* Cobban, 1951, in dorsoventral section. Abbreviations: **dm,** shell diameter; **uw,** umbilical width; **WER,** whorl expansion rate; **wh,** whorl height; **ww,** whorl width.

sponding to a shell diameter of 3–5 mm. We selected an average value of 4 mm as our point of comparison and obtained the values for the four ratios at this diameter by interpolation, using the plots of the ratios versus log diameter. The neanic stage is generally interpreted as the transition from a planktonic mode of life to a more adultlike, possibly demersal, mode of life near the bottom (Westermann, 1996; Tsujita and Westermann, 1998; Walton and Korn, 2017).

3. Submature stage (fig. 1A–U, arrows). In *Scaphites whitfieldi*, the shell uncoils at the end of ontogeny and forms a shaft and recurved hook. This sequence reflects the growth of the reproductive organs and the attainment of maturity. The adult animal may have lived close to the bottom in well-oxygenated environments (Landman et al.,

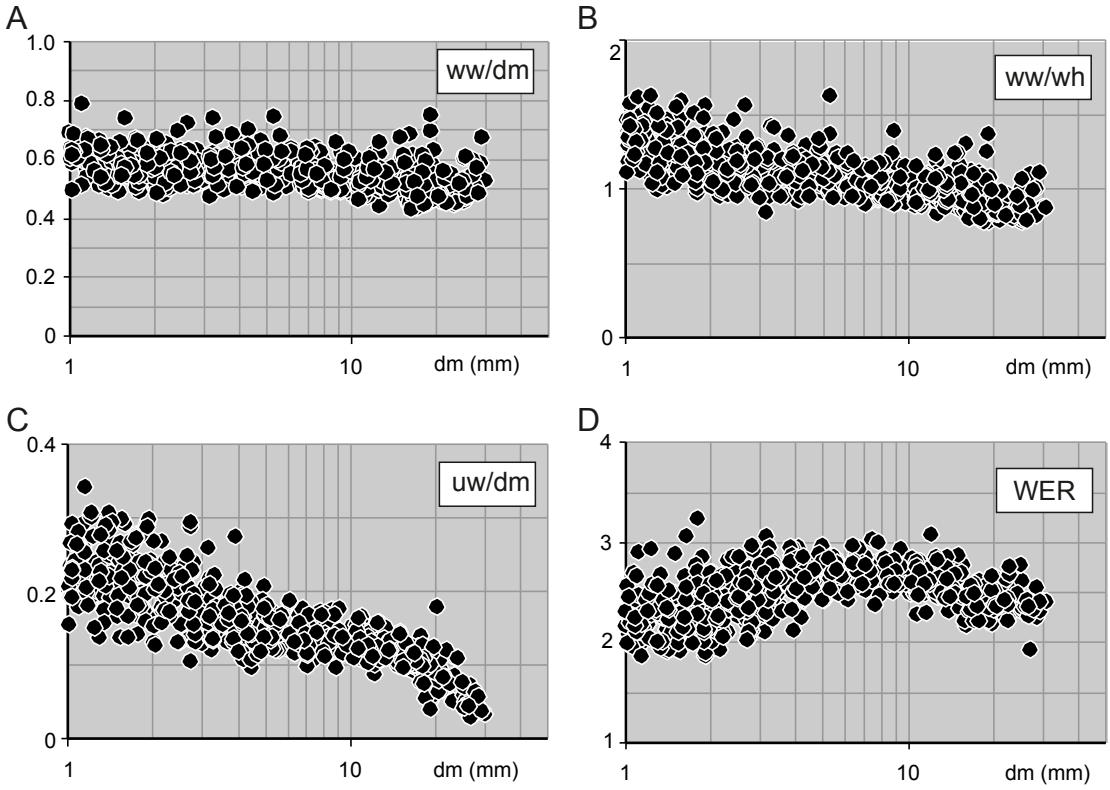

FIGURE 5. Ontogenetic trajectories of all specimens of *Scaphites whitfieldi* Cobban, 1951, used in the study. The ratios are plotted against log diameter (dm).

2012a). The morphogenetic countdown toward maturity begins at the point at which the shell departs from the spiral coil and develops into the shaft. It approximately coincides with the position of the last septum (end of the phragmocone) and represents the submature stage. The diameter at this point ranges from 10.4 to 30.8 mm in our sample, which closely matches the range of 12 to 34 mm for adult phragmocones of this species, as reported by Landman (1987: figs. 63, 77). It corresponds to 4.0 to 5.5 whorls in our sample, which closely matches the range of 3.6 to 4.3 whorls for this species, as reported by Landman (1987: fig. 71), taking into account the fact that his values did not include the number of whorls in the ammonitella (0.75 whorls).

To assess intraspecific variation through ontogeny, box-and-whiskers plots were produced for the three growth stages (for a recent discussion about the use of this technique, see Korn and Klug, 2007; Monnet et al., 2010; and De Baets et al., 2015). The thickness of the boxes represents the middle two quartiles and the whiskers extend to the maximum and minimum values. Results were compared using F and modified student's t tests [level of confidence (α) = 0.01]. In addition, we reported the coefficient of variation [CV = (SD/mean) X 100]. Morphological disparity was assessed by a principal components analysis (PCA) of three of the shell

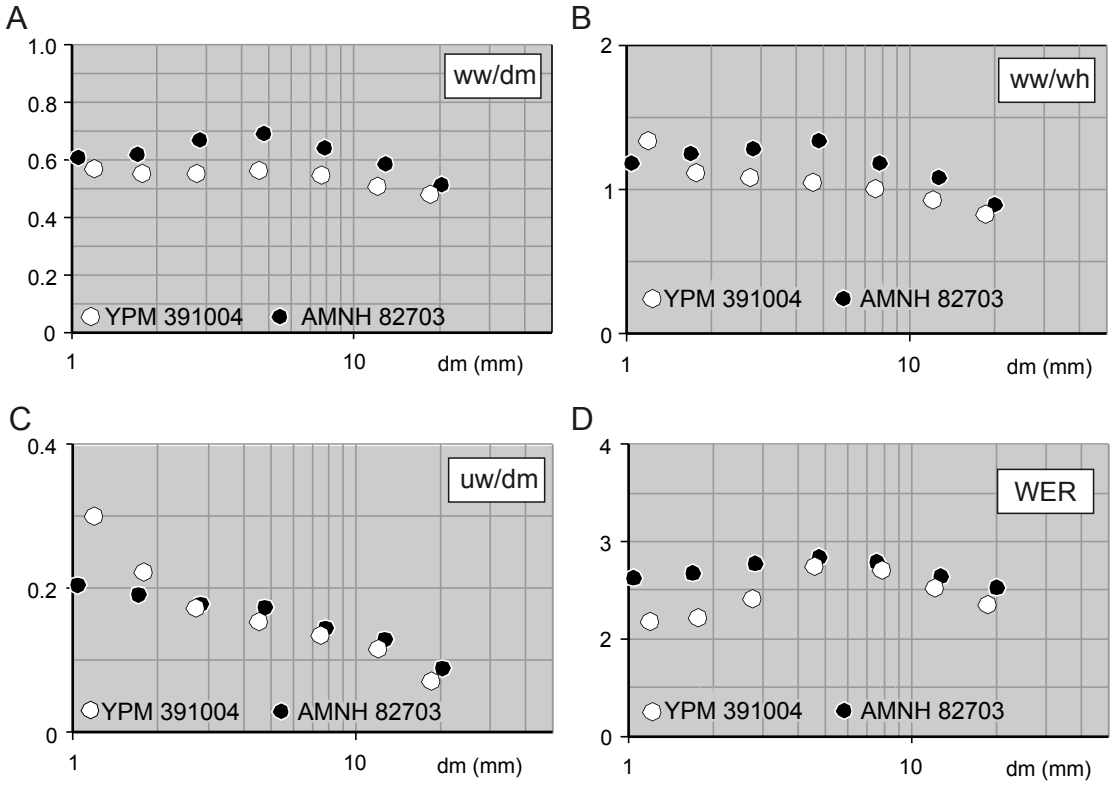

FIGURE 6. Ontogenetic trajectories of two specimens of *Scaphites whitfieldi* Cobban, 1951. The ratios are plotted against log diameter (dm). The specimen with the white dots (YPM 391004) shows the ontogenetic pattern typical of specimens from the siltstone and the specimen with black dots (AMNH 82703) shows the ontogenetic pattern typical of specimens from the shale.

parameters (ww/dm, uw/dm, and WER). In addition, the sums of the ranges (SOR) and variances (SOV) were calculated to provide a more complete picture (for a description of this method, see Wills, 2001). All results are reported in the tables in appendix 1.

RESULTS

1. Ontogenetic Trajectory

In general, the values of the shell parameters (ww/dm, ww/wh, uw/dm, and WER) decrease through ontogeny (figs. 5, 6, appendix 1: table 1). In these descriptions, we follow the morphological terminology of Korn (2012), as indicated by quotation marks. The shell is initially "pachyconic" (ww/dm > 0.6) and then becomes more "discoidal" (ww/dm = 0.4–0.6). The whorl cross section is initially "weakly depressed" (ww/wh >1.0) up to dm ≈ 10 mm and then becomes "weakly compressed" (ww/wh = 0.8–1.0). The umbilicus is initially "narrow" (uw/dm >0.15) and then becomes "very narrow" (uw/dm = 0.05–0.10). The whorl expansion rate (WER) shows a biphasic development. It increases from a "very high" value of ≈ 2.5 to an "extremely high" value of 2.5–3.0 at 5 mm ≤ dm ≤ 8 mm and subsequently declines to a "very high" value again of ≈ 2.5.

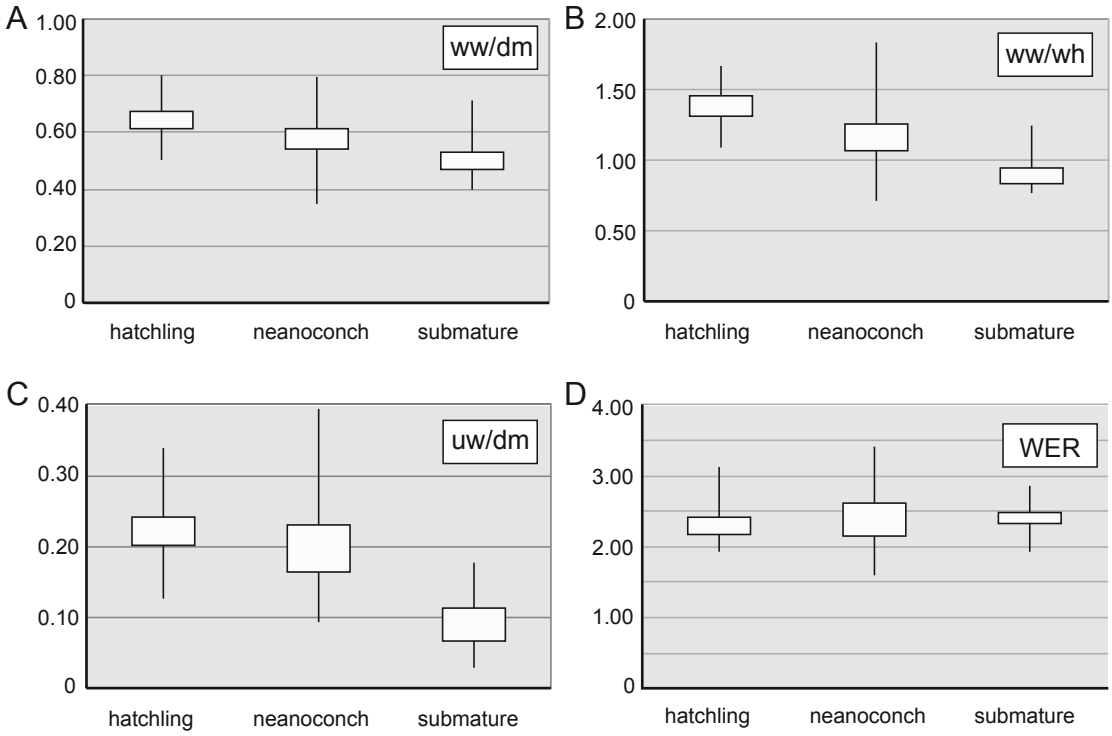

FIGURE 7. Box and whiskers plot showing the intraspecific variation of each shell parameter at three ontogenetic stages. The thickness of the boxes represents the middle two quartiles and the whiskers extend to the maximum and minimum values.

In summary, the shell becomes more discoidal through ontogeny with a narrower umbilicus and a more compressed whorl section. The rate of expansion initially increases and then decreases.

2. Intraspecific variation assessed by univariate methods

A comparison of the three ontogenetic stages using box-and-whiskers plots for the entire sample reveals that the maximum variation occurs in the neanoconch compared with the hatchling or submature stage (fig. 7, appendix 1: tables 4, 7). Based on the F test, the variation in all four parameters is statistically significantly higher in the neanoconch than in the hatchling. In addition, the variation in three of the parameters (ww/wh, uw/dm, and WER) is statistically significantly higher in the neanoconch than in the submature stage. In contrast, the variation is only statistically significantly different between the hatchling and the submature stage in one of the four parameters (WER).

We also compared the values of the parameters for the hatchling, neanoconch, and submature stage between the sample from siltstone (n = 63) and the sample from shale (n = 40) (fig. 8, appendix 1: tables 2, 5, 7). In the hatchling, the variation is not significantly different between these two samples. The means of ww/wh and uw/dm are significantly higher in the siltstone than in the shale and the mean of WER is significantly higher in the shale than in the siltstone. In the neanoconch, the variation in uw/dm is significantly different between the two

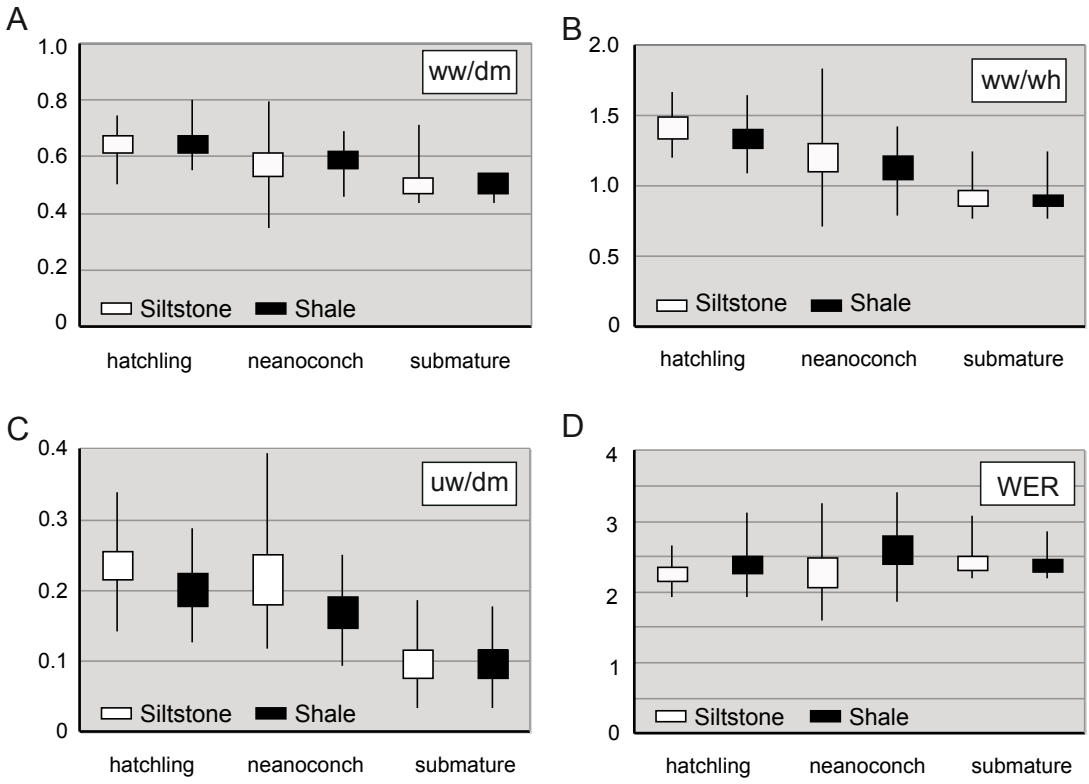

FIGURE 8. Box and whiskers plot showing the intraspecific variation of each shell parameter at three ontogenetic stages in the samples from the two different facies. The thickness of the boxes represents the middle two quartiles and the whiskers extend to the maximum and minimum values.

samples. The mean of uw/dm is significantly higher in the siltstone and the mean of WER is significantly higher in the shale. In the submature stage, the variation in two of the parameters (ww/dm and ww/wh) is significantly different between the two samples. The means of ww/dm and WER are significantly higher in the shale than in the siltstone.

In addition, we compared the values of the parameters for all three ontogenetic stages between a sample of specimens (n = 12) from a single concretion (B176a) versus a sample of specimens (n = 16) from the same site, but from multiple concretions (B176) (fig. 9, appendix 1: tables 3, 6, 7). With respect to hatchlings, the variation is not significantly different between the sample from multiple concretions and the sample from a single concretion. In terms of means, the values of ww/dm and ww/wh of the hatchlings are significantly higher in the sample from multiple concretions than from a single concretion. With respect to the neanoconch, the variation of uw/dm and WER is significantly higher in the sample from multiple concretions than from a single concretion. With respect to the submature stage, the variation of ww/dm, ww/wh, and WER is significantly higher in the sample from multiple concretions than from a single concretion. In terms of means, for both the neanoconch and submature stage, the values of ww/dm, ww/wh, uw/dm, and WER are not significantly different in the sample from multiple concretions than from a single concretion.

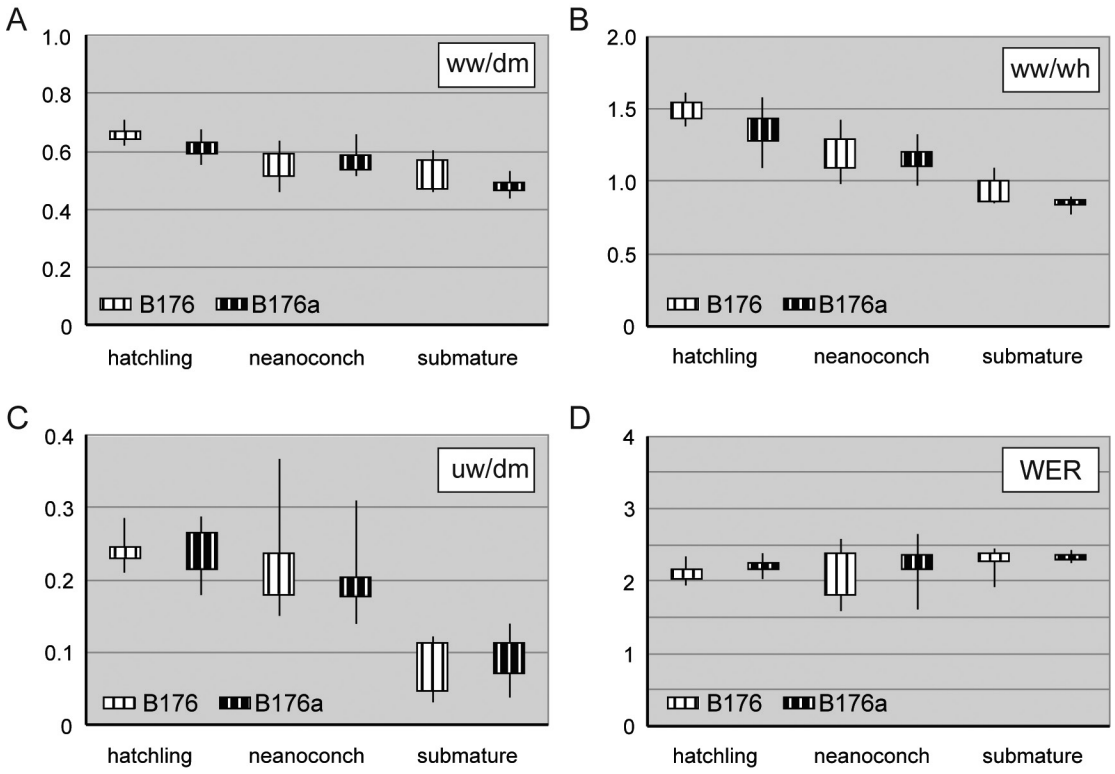

FIGURE 9. Box and whiskers plot showing the intraspecific variation of each shell parameter at three ontogenetic stages in the sample from a single concretion (B176a) versus the sample from multiple concretions (B176). The thickness of the boxes represents the middle two quartiles and the whiskers extend to the maximum and minimum values.

Finally, we compared the values of the three ontogenetic stages between microconchs (n = 4) and macroconchs (n = 4) from the same concretion (B192s). Based on the F test and the student's t test, the results are not statistically significantly different for any of the parameters, probably as a result of the small size of the sample.

3. Disparity

A morphospace of the three growth stages (hatchling, neanoconch, and submature) was created by performing a principal components analysis (PCA) using three of the four shell parameters (ww/dm, uw/dm, and WER) (fig. 10A–C). We excluded ww/wh because it is strongly correlated with ww/dm. The first two principal components represent 86.6% of the total variation. The arrows in the figure indicate increasing values of the three parameters. The values for each ontogenetic stage are highlighted with different colors for the two facies. In addition, the values for all of the ontogenetic stages are plotted in each figure to provide a picture of the complete ontogenetic morphospace.

A clear morphological separation is observed among the three growth stages. During ontogeny, the values shift toward the lower left of the diagram, that is, toward lower values of

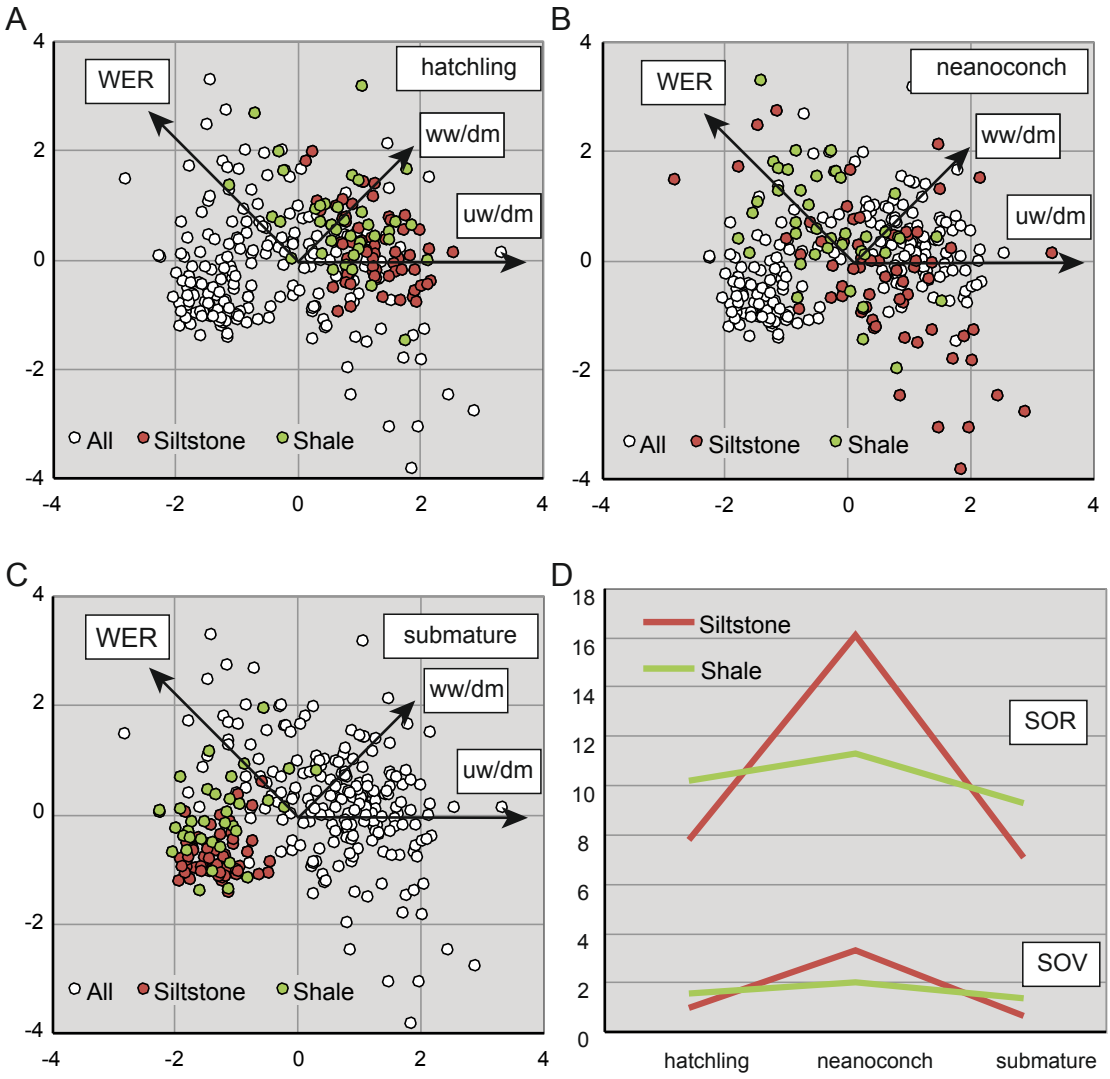

FIGURE 10. Morphospace showing the ontogeny of all specimens with the two facies highlighted. **A.** Hatchling. **B.** Neanoconch. **C.** Submature stage. **D.** Sums of the ranges (SOR) and variances (SOV) at each ontogenetic stage with the two facies highlighted.

ww/dm (fig. 10A–C). The hatchling (fig. 10A) is more depressed and openly umbilicate (high ww/dm, high uw/dm). In the neanoconch (fig. 10B), the disparity increases markedly, especially in terms of WER. Subsequently, the disparity contracts at the submature stage (fig. 10C).

The three growth stages are also separated according to facies (fig. 10A–C). In general, the specimens from the siltstone occupy lower regions of the morphospace, implying that they are more compressed than those in the shale. In the neanoconch, specimens from the siltstone also exhibit much lower values of WER than their counterparts in the shale. The differences in disparity between growth stages and facies are also apparent when the sums of the ranges

(SOR) and variances (SOV) are calculated (fig. 10D). Specimens in the siltstone exhibit a greater change in disparity through ontogeny, with a marked peak in the neanoconch. In the hatchling and submature stage, the disparity is lower in the siltstone than in the shale, but the reverse is true in the neanoconch—the disparity is higher in the siltstone than in the shale.

DISCUSSION

Plots of the ontogenetic trajectory of *Scaphites whitfieldi* reveal that the shell becomes more discoidal through ontogeny with a narrower umbilicus and a more compressed whorl section (figs. 5, 6). This trend also appears in the principal components analysis in which the values shift toward the lower left of the diagram during ontogeny, that is, toward lower values of ww/dm (fig. 10A–C). Many Mesozoic ammonites follow a similar pattern of increasing compression through ontogeny (Smith, 1897, 1898, 1900; Tanabe and Shigeta, 1987: fig. 5). This ontogenetic change in the degree of compression is consistent with hydrodynamic expectations related to increase in the size of the animal (Jacobs and Chamberlain, 1996). The spherical shape of the shell at hatching minimizes surface area and skin friction drag. However, as size increases, a more compressed shell shape confers better hydrodynamic efficiency.

A comparison of the parameters for the three ontogenetic stages reveals that the morphological variation is relatively low in the hatchling (figs. 7, 10A–C). Several studies have investigated the intraspecific variation in the ammonitella with respect to its diameter and angular length of the body chamber (ammonitella angle), as summarized by DeBaets et al. (2015: fig. 5.6, table 5.2). In Late Cretaceous scaphites, the coefficient of variation of the ammonitella diameter ranges from 4% to 6% and the coefficient of variation of the ammonitella angle ranges from 3% to 4% (Landman, 1987). In Middle Jurassic oppeliids, the coefficients of variation of these two parameters average 7% and 4%, respectively (Rouget and Neige, 2001). The coefficients of variation of the four parameters in our study are generally less than 10% (appendix 1: table 7). The low morphological variation of the newly hatched shell, especially with respect to the neanoconch (see below), may reflect developmental constraints imposed by morphological integration. The dimensions of the initial chamber and the ammonitella are closely correlated, so that the newly hatched animal is neutrally buoyant (Landman et al. 1996; De Baets et al. 2015).

The variation in morphology is much higher in the neanoconch (fig. 7). Based on the F test, with respect to the hatchling, the variation in all four parameters is statistically significantly higher in the neanoconch and, with respect to the submature stage, the variation in three of the parameters (ww/wh, uw/dm, and WER) is statistically significantly higher in the neanoconch (appendix 1: table 4). The difference between the neanoconch and the other two stages is also apparent in the principal components analysis, in which the disparity increases markedly in the neanoconch (fig. 10A–C).

Many morphological changes occur at the end of the neanic stage (fig. 2E, F) and involve whorl width, whorl height, umbilical width, and rate of whorl expansion as well as ornamentation, sutural complexity, and septal spacing (Bucher et al., 1996). This nearly simultaneous explosion of morphological changes contributes to the high degree of variation observed at

this point. Previous studies have similarly alluded to more variation in juveniles than adults referring to the juveniles as "plastic" (Arkell et al., 1957: L110). However, the juveniles in these other studies are generally larger than 4 mm, so that these results are difficult to compare with our own (e.g., dm ≤40 mm in Monnet et al., 2012; dm = 16 mm in De Baets et al., 2013). However, it is important to note that the morphological changes at the end of the neanic stage occur over a range of size (dm = 3–5 mm). Therefore, at dm = 4 mm (our target size), it is possible that some individuals may have already undergone these changes whereas others may not have, thus inflating the degree of variation in our analysis. To resolve this issue in the future, it is critical to examine each ontogenetic trajectory individually to pinpoint the exact size at which the morphological changes occur.

The degree of variation decreases at the submature stage. This is apparent in the box and whiskers plots (fig. 7) as well as in the disparity analysis (fig. 10A–C). The contraction of morphological variation at this stage reflects the canalization leading to maturity, which involves its own set of morphological changes, including the uncoiling of the body chamber (Landman, 1989). The decrease in variation at the submature stage in our study is particularly striking because, unlike the hatchling (dm = 1 mm), for example, the submature stage encompasses a wide range of size and whorl number (dm = 10.4–30.8 mm; number of whorls = 4.0–5.5). In more advanced scaphite species in the genus *Hoploscaphites*, Landman et al. (2010) also noted that specimens converge on the same morphology at maturity (sorted out according to dimorph), despite the wide size spectrum over which they mature, probably reflecting a concomitant variation in age. A reduction in morphological variation at maturity is a common pattern in ammonites (Tanabe and Shigeta, 1987: 172–173, figs. 7, 8; De Baets et al., 2013: fig. 6).

The samples of *Scaphites whitfieldi* in our study are from two facies, shale and siltstone. These two facies are principally distinguished by the type of sediment. However, differences in sediment type are usually associated with differences in other environmental parameters including turbidity, turbulence, light, nutrients, depth, and distance from shore (De Baets et al. 2015). Many ammonite studies have demonstrated a correlation between shell morphology and facies, especially in ammonites that presumably lived close to the bottom. For example, Batt (1989) demonstrated a correlation between shell morphology and facies at the generic level in the Cenomanian of the U.S. Western Interior, and Wilmsen and Mosavinia (2011) demonstrated a correlation between shell morphology and facies at the species level in the Cenomanian of Iran. Such studies are predicated on the assumption that the distribution of ammonites reflects their original habitat rather than an artifact due to postmortem drifting. The scaphites in our study are well preserved with intact body chambers, suggesting that they lived and died in the same area in which they are preserved. In his study of scaphites in the Turonian of Hokkaido, Japan, Tanabe (1979) also concluded that scaphites, unlike phylloceratids and lytoceratids that lived in deeper water, did not experience much postmortem drift.

A comparison of the samples in the shale and siltstone reveals significant differences in several shell parameters (fig. 8, appendix 1: table 2). In the submature stage, the specimens from the siltstone occupy lower regions of the morphospace, implying that they are more compressed than those in the shale (fig. 10A–C). The more compressed shell shape of the specimens in the siltstone is consis-

tent with hydrodynamic expectations. At higher Reynolds numbers (≈ higher rates of flow) characteristic of higher-energy environments, the coefficient of drag is lower in more-compressed forms due to their smaller cross-sectional area. Jacobs et al. (1994) reached a similar conclusion in their study of *Scaphites whitfieldi* from the Carlile Shale of South Dakota in which they utilized a flow tank to measure coefficient of drag versus Reynolds number on casts of actual specimens.

In addition, as shown by the sums of the ranges (SOR) and variances (SOV), the disparity at the submature stage is lower in the siltstone than in the shale (fig. 10D). The implication is that the higher-energy environment represented by the siltstone imposes more intense selection pressures for hydrodynamically optimal shell shapes at this stage of development. In contrast, the environment represented by the shale poses fewer constraints and is more permissive with respect to this parameter. Westermann (1996) made a similar argument about variation in shell shape and ammonite mode of life. He postulated that variation in shell shape related to streamlining is higher in forms like planktic drifters in which streamlining is unimportant compared to demersal swimmers in which it is essential.

In contrast, the disparity in the neanoconch is much higher in the siltstone than in the shale, especially with respect to the parameter WER (fig. 10D). As alluded to earlier, this may partly reflect our choice of a single target size (dm = 4 mm) for the end of the neanic stage. Furthermore, it is possible that the siltier, more nearshore environment was also more spatially heterogeneous than the muddier, more offshore environment. This increased spatial heterogeneity may have resulted in more variation in the rate of growth among individuals, due perhaps to local differences in the availability of nutrients. As a consequence, the end of the neanic stage in this environment may have occurred over a broader range of sizes than in the muddier, more offshore environment, contributing to a greater degree of morphological variation in our study. Indeed, environmental factors such as nutrients and temperature have an enormous impact on the rate of growth of cephalopods in general (De Baets et al., 2015).

The observed differences in the values of the shell parameters between samples from the two facies (appendix 1: table 2) imply that the populations inhabiting each of these facies probably did not interbreed. If the sites are more or less time equivalent, at least as inferred from biostratigraphic data, these differences suggest that the scaphites did not migrate over long distances. Instead, they may have remained at their respective sites throughout their lives. Several studies corroborate this hypothesis. Cochran et al. (2003) investigated the strontium isotopes in adults of a species of *Hoploscaphites* from the Maastrichtian of South Dakota. They discovered that the strontium isotope ratios of specimens from different sites ware also different. Provided that these sites are time equivalent, this implies that the animals did not migrate between sites. Similarly, Yahada and Wani (2013) studied a species of *Scaphites* from two sites in the Turonian of Hokkaido, Japan. The specimens from the two sites differed in their degree of whorl compression, leading the authors to conclude that the two populations did not interbreed. In addition, Landman et al. (2012b) analyzed the carbon and oxygen isotopic composition of a species of *Hoploscaphites* at cold methane seep deposits in the Campanian of South Dakota. Their data revealed that the scaphites incorporated isotopi-

cally light methane-derived carbon in their shells, suggesting that the animals did not migrate, but spent their entire lives at the seep.

We compared the values of the parameters for all three ontogenetic stages between a sample of specimens from a single concretion versus a sample of specimens from the same site, but from multiple concretions (fig. 9, appendix 1: tables 3, 6). In the neanoconch and submature stage, the variation of most of the shell parameters is significantly higher in the sample from multiple concretions than that from a single concretion. Undoubtedly, this reflects the difference in the source of material and the amount of time averaging. A single concretion draws on a more limited source of material and represents less time averaging. In their study of fossiliferous concretions from the Pierre Shale, Landman and Klofak (2012: 690) estimated that such concretions formed during relatively short periods of time (<10 years) and, as a result, "the examination of specimens in a single concretion provides more reliable data for determining the range of variation of a species than examination of specimens from different horizons, even if they are in the same biostratigraphic zone." For example, to determine the size difference between dimorphs in the same species of *Hoploscaphites*, Landman et al. (2010) examined samples from single concretions. Finally, a comparison of the values of the three ontogenetic stages between microconchs and macroconchs in the same concretion also reveals no statistically significant difference for any of the parameters, although this may reflect the small size of the sample.

CONCLUSIONS

Investigation of the ontogeny of the Late Cretaceous ammonite *Scaphites whitfieldi* reveals that the shell becomes more discoidal through ontogeny with a narrower umbilicus and a more compressed whorl section. This ontogenetic change in the degree of compression is consistent with hydrodynamic expectations related to the increase in the size of the shell. The variation in morphology is much higher in the neanoconch than in the hatchling or submature stage. The shell exhibits many morphological changes at this point that affect the whorl width, whorl height, umbilical width, and rate of whorl expansion as well as ornamentation, sutural complexity, and septal spacing. These changes are consistent with the hypothesis that the end of the neanic stage represents a transition in the life history of the animal to a more demersal mode of life, followed by a canalization of morphology toward maturity. However, to more fully explore the variation at the end of the neanic stage, it is critical in the future to examine individual ontogenetic trajectories to pinpoint the exact diameter at which the morphological changes occur. A comparison of the samples in the shale and siltstone reveals significant differences in several shell parameters. In general, the specimens from the siltstone occupy lower regions of the morphospace, implying that they are more compressed than those in the shale. This difference may be related to more intense selection pressures for improved hydrodynamic efficiency in the higher energy environment represented by the siltstone.

ACKNOWLEDGMENTS

We thank Steve Thurston (AMNH) for help in preparing the figures, Mariah Slovacek (AMNH) for help in preparing the dorsoventral sections, Bushra Hussaini (AMNH) for help in curating the specimens, and Susan Butts (YPM) and K.C. McKinney (USGS) for help in arranging the loan of material. An earlier version of this manuscript was reviewed by James D. Witts (AMNH), Melanie J. Hopkins (AMNH), and Daniel A. Stephen (Utah Valley University), all of whom made many helpful suggestions that improved the quality of the manuscript. C.K. acknowledges the Annette Kade Charitable Trust Fund (AMNH) and the Elsa Neumann Foundation (Humboldt Universität zu Berlin) for supporting her visit to the AMNH.

REFERENCES

Arkell, W.J., B. Kummel, and C.W. Wright. 1957. Mesozoic Ammonoidea. *In* W.J. Arkell et al., Treatise on invertebrate paleontology, part L, Mollusca 4, Cephalopoda, Ammonoidea: L8–L490. New York: Geological Society of America.

Batt, R.J. 1989. Ammonite shell morphotype distribution in the Western Interior Greenhorn Sea and some paleoecological implications. Palaios 4: 32–42.

Branco, W. 1879–1880. Beiträge zur Entwickelungs Geschichte der fossilen Cephalopoden. Palaeontographica (Stuttgart) 26 (1879): 15–50; 27 (1880): 17–81.

Bucher, H., N.H. Landman, S.M. Klofak, and J. Guex. 1996. Mode and rate of growth in ammonoids. *In* N.H. Landman, K. Tanabe, and R.A. Davis (editors), Ammonoid paleobiology: 407–461. New York: Plenum Press.

Cobban, W.A. 1951. Scaphitoid cephalopods of the Colorado Group. U.S. Geological Survey Professional Paper 239, 42 pp.

Cobban, W.A., C.E. Erdmann, R.W. Lemke, and E.K. Maughan. 1976. Type sections and stratigraphy of members of the Blackleaf and Marias River Formations (Cretaceous) of the Sweetgrass Arch, Montana. U.S. Geological Survey Professional Paper 974, 66 pp.

Cobban, W.A., I. Walaszczyk, J.D. Obradovich, and K.C. McKinney. 2006. A USGS zonal table for the Upper Cretaceous (middle Cenomanian–Maastrichtian) of the Western Interior of the United States based on ammonites, inoceramids, and radiometric ages. U.S. Geological Survey Open-File Report 2006–1250.

Cochran, J.K., N.H. Landman, K.K. Turekian, A. Michard, and D.P. Schrag. 2003. Paleoceanography of the Late Cretaceous (Maastrichtian) Western Interior Seaway of North America: evidence from Sr and O isotopes. Palaeogeography, Palaeoclimatology, Palaeoecology 191 (1): 45–64.

Cooper, M.R. 1994. Towards a phylogenetic classification of the Cretaceous ammonites. III. Scaphitaceae. Neues Jahrbuch für Geologie und Palaeontologie Abhandlungen 193 (2): 165–193.

Dagys, A.S., and W. Weitschat. 1993. Extensive intraspecific variation in a Triassic ammonoid from Siberia. Lethaia 26 (2): 113–121.

De Baets, K., C. Klug, and C. Monnet. 2013. Intraspecific variability through ontogeny in early ammonoids. Paleobiology 39 (1): 75–94.

De Baets, K., et al. 2015. Ammonoid intraspecific variability. *In* C. Klug, D. Korn, K. De Baets, I. Kruta, and R.H. Mapes (editors) Ammonoid paleobiology: from anatomy to ecology: 359–426. Dordrecht: Springer.

Druschits, V.V., and L.A. Doguzhaeva. 1981. Ammonites under the electron microscope. Moscow: Moscow University Press. [in Russian]

Hyatt, A. 1894. Phylogeny of an acquired characteristic. Proceedings of the American Philosophical Society 32 (143): 349–647.

Jacobs, D.K., and J.A. Chamberlain, Jr. 1996. Buoyancy and hydrodynamics in ammonoids. *In* N.H. Landman, K. Tanabe, and R.A. Davis (editors), Ammonoid paleobiology: 169–224. New York: Plenum Press.

Jacobs, D.K., N.H. Landman, and J.A. Chamberlain, Jr. 1994. Ammonite shell shape covaries with facies and hydrodynamics: iterative evolution as a response to changes in basinal environment. Geology 22 (10): 905–908.

Kant, R., and J. Kullmann. 1973. "Knickpunkte" in allometrischen Wachstum von Cephalopoden-Gehausen. Neues Jahrbuch für Geologie und Palaeontologie Abhandlungen 142 (1): 97–114.

Klug, C., M. Zatoń, H. Parent, B. Hostettler, and A. Tajika. 2015. Mature modifications and sexual dimorphism. *In* C. Klug, D. Korn, K. De Baets, I. Kruta, and R.H. Mapes (editors), Ammonoid paleobiology: from anatomy to ecology: 253–320. Dordrecht: Springer.

Korn, D. 2012. Quantification of ontogenetic allometry in ammonoids. Evolution and Development 14 (6): 501–514.

Korn, D., and C. Klug. 2007. Conch form analysis, variability, morphological disparity, and mode of life of the Frasnian (Late Devonian) ammonoid *Manticoceras* from Coumiac (Montagne Noire, France). *In* N.H. Landman, R.A. Davis, and R.H. Mapes (editors), Cephalopods, present and past: new insights and fresh perspectives: 57–85. New York: Springer.

Korn, D., and C. Klug. 2012. Palaeozoic ammonoids–diversity and development of conch morphology. *In* J.A. Talent, (editor), Earth and life: global biodiversity, extinction intervals and biogeographic perturbations through time: 491–534. Dordrecht: Springer.

Landman, N.H. 1987. Ontogeny of Upper Cretaceous (Turonian-Santonian) scaphitid ammonites from the Western Interior of North America: systematics, developmental patterns, and life history. Bulletin of the American Museum of Natural History 185 (2): 117–241.

Landman, N.H. 1988. Heterochrony in ammonites. *In* M.L. McKinney (editor), Heterochrony in evolution: a multidisciplinary approach: 159–179. New York: Plenum Press.

Landman, N.H. 1989. Iterative progenesis in Upper Cretaceous ammonites. Paleobiology 15 (1): 95–117.

Landman, N.H., and S.M. Klofak. 2012. Anatomy of a concretion: life, death, and burial in the Western Interior Seaway. Palaios 27: 672–693.

Landman, N.H., and K.M. Waage. 1982. Terminology of structures in embryonic shells of Mesozoic ammonites. Journal of Paleontology 56 (5): 1293–1295.

Landman, N.H., and K.M. Waage. 1993. Scaphitid ammonites of the Upper Cretaceous (Maastrichtian) Fox Hills Formation in South Dakota and Wyoming. Bulletin of the American Museum of Natural History 215: 1–257.

Landman, N.H., K. Tanabe, and Y. Shigeta. 1996. Ammonoid embryonic development. *In* N.H. Landman, K. Tanabe, and R.A. Davis (editors), Ammonoid paleobiology: 343–405. New York: Plenum Press.

Landman, N.H., W.J. Kennedy, W.A. Cobban, and N.L. Larson. 2010. Scaphites of the "*nodosus* group" from the Upper Cretaceous (Campanian) of the Western Interior of North America. Bullletin of the American Museum of Natural History 342: 1–242.

Landman, N.H., W.A. Cobban, and N.L. Larson. 2012a. Mode of life and habitat of scaphitid ammonites. Geobios 45: 87–98.

Landman, N.H., et al. 2012b. Methane seeps as ammonite habitats in the U.S. Western Interior Seaway revealed by isotopic analyses of well-preserved shell material. Geology 40 (6): 507–510.

Landman, N.H., A.G. Plint, and I. Walaszczyk. 2017. Scaphitid ammonites from the Upper Cretaceous (Coniacian-Santonian) Western Canada Foreland Basin. *In* Landman, N.H., A.G. Plint, and I.

Walaszczyk (editors), Allostratigraphy and biostratigraphy of the Upper Cretaceous (Coniacian-Santonian) Western Canada Foreland Basin. Bulletin of the American Museum of Natural History 414: 105–172.

McGookey, D.P., et al. 1972. Cretaceous System. *In* Geologic atlas of the Rocky Mountain region: 190–228. Denver: Rocky Mountain Association of Geologists.

Monnet, C., H. Bucher, M. Wasmer, and J. Guex. 2010. Revision of the genus *Acrochordiceras* Hyatt, 1877 (Ammonoidea, Middle Triassic): morphology, biometry, biostratigraphy and intraspecific variability. Palaeontology 53 (5): 961–996.

Monnet, C., H. Bucher, J. Guex, and M. Wasmer. 2012. Large-scale evolutionary trends of Acrochordiceratidae Arthaber, 1911 (Ammonoidea, Middle Triassic) and Cope's Rule. Palaeontology 55 (1): 87–107.

Moseley, H. 1838. On the geometrical forms of turbinated and discoid shells. Philosophical Transactions of the Royal Society of London: 351–370.

Naglik, C., et al. 2015. Growth trajectories of some major ammonoid sub-clades revealed by serial grinding tomography data. Lethaia 48 (1): 29–46.

Raup, D. 1967. Geometric analysis of shell coiling: coiling in ammonoids. Journal of Paleontology 41: 43–65.

Rouget, I., and P. Neige. 2001. Embryonic ammonoid shell features: intraspecific variation revisited. Palaeontology 44: 53–64.

Schindewolf, O.H. 1954. On development, evolution, and terminology of ammonoid suture line. Harvard University Museum of Comparative Zoology Bulletin 112 (3): 217–237.

Smith, J.P. 1897. The development of *Glyphioceras* and the phylogeny of the Glyphioceratidae. Proceedings of the California Academy of Sciences 1: 105–128.

Smith, J.P. 1898. The development of *Lytoceras* and *Phylloceras*. Proceedings of the California Academy of Sciences 1: 129–232.

Smith, J.P. 1900. The development and phylogeny of *Placenticeras*. Proceedings of the California Academy of Sciences 3: 181–232.

Tajika, A., N. Morimoto, R. Wani, and C. Klug. 2018. Intraspecific variation in cephalopod conch changes during ontogeny: perspectives from three-dimensional morphometry of *Nautilus pompilius*. Paleobiology 44 (1): 118–130.

Tanabe, K. 1979. Palaeoecological analysis of ammonoid assemblages in the Turonian *Scaphites* facies of Hokkaido, Japan. Palaeontology 22 (3): 609–630.

Tanabe, K., and Y. Shigeta. 1987. Ontogenetic shell variation and streamlining of some Cretaceous ammonites. Transactions and Proceedings of the Palaeontological Society of Japan, New Series 147: 165–179.

Thompson, D.W. 1917. On growth and form. London: Cambridge University Press, 1116 pp.

Tsujita, C.J., and G.E.G. Westermann. 1998. Ammonoid habitats and habits in the Western Interior Seaway: a case study from the Upper Cretaceous Bearpaw Formation of southern Alberta, Canada. Palaeogeography, Palaeoclimatology, Palaeoecology 144: 135–160.

Walton, S.A., and D. Korn. 2017. Iterative ontogenetic development of ammonoid conch shapes from the Devonian through to the Jurassic. Palaeontology 60 (5): 703–726.

Westermann, G.E.G. 1996. Ammonoid life and habitat. *In* N.H. Landman, K. Tanabe, and R.A. Davis, (editors), Ammonoid paleobiology. New York: Plenum Press.

Wiedmann, J., and J. Kullmann. 1980. Ammonoid sutures in ontogeny and phylogeny. *In* M.R. House and J.R. Senior (editors) The Ammonoidea: 215–255. New York: Academic Press.

Wills, M.A. 2001. Morphological disparity: a primer. *In* Fossils, phylogeny, and form: 55–144. Boston: Springer.

Wilmsen, M., and A. Mosavinia. 2011. Phenotypic plasticity and taxonomy of *Schloenbachia varians* (J. Sowerby, 1817) (Cretaceous Ammonoidea). Paläontologische Zeitschrift 85: 169–184.

Yacobucci, M. 2004. Buckman's Paradox: variability and constraints on ammonoid ornament and shell shape. Lethaia 37 (1): 57–69.

Yahada, H., and R. Wani. 2013. Limited migration of scaphitid ammonoids: evidence from the analyses of shell whorls. Journal of Paleontology 87: 406–412.

APPENDIX 1

Means, Standard Deviations, and Coefficients of Variation for ww/dm, ww/wh, uw/dm, and WER of Sampled Material

Boldface p-value entries indicate significant differences ($\alpha = 0.01$). For terminology, see figure 4.

1. Mean values for all specimens ($n = 103$).

	ww/dm	ww/wh	uw/dm	WER
Hatchling	0.65	1.38	0.22	2.31
Neanoconch	0.58	1.17	0.20	2.39
Submature	0.51	0.90	0.09	2.41

2. Mean values for specimens from siltstone ($n = 63$) and from shale ($n = 40$).

	ww/dm			ww/wh		
	Siltstone	Shale	p	Siltstone	Shale	p
Hatchling	0.64	0.65	5.34E-01	1.41	1.34	**5.72E-03**
Neanoconch	0.58	0.59	5.13E-01	1.20	1.12	1.11E-02
Submature	0.50	0.53	**7.45E-03**	0.88	0.94	1.22E-02

	uw/dm			WER		
Hatchling	0.23	0.20	**3.09E-04**	2.26	2.40	**1.35E-03**
Neanoconch	0.22	0.17	**2.94E-06**	2.40	2.57	**2.23E-05**
Submature	0.09	0.09	5.49E-01	2.35	2.50	**8.67E-06**

3. Mean values for specimens from multiple concretions (176; $n = 12$) and from a single concretion (176a; $n = 16$).

	ww/dm			ww/wh		
	176	176a	p	176	176a	p
Hatchling	0.66	0.62	**2.15E-03**	1.49	1.36	**1.96E-03**
Neanoconch	0.55	0.57	3.87E-01	1.19	1.15	4.45E-01
Submature	0.52	0.48	6.62E-02	0.92	0.86	4.22E-02

	uw/dm			WER		
Hatchling	0.24	0.24	9.09E-01	2.11	2.21	3.58E-02
Neanoconch	0.23	0.19	1.04E-01	2.05	2.31	4.06E-02
Submature	0.08	0.09	6.39E-01	2.31	2.32	8.16E-01

4. Standard deviations for ww/dm, ww/wh, uw/dm, and WER for all specimens (n = 103).

	ww/dm		ww/wh	
		p		p
Neanoconch vs. hatchling	0.07 vs. 0.05	**1.68E-03**	0.16 vs. 0.12	**3.84E-04**
Hatchling vs. submature	0.05 vs. 0.04	1.01E-01	0.12 vs. 0.10	7.43E-02
Neanoconch vs. submature	0.07 vs. 0.04	4.96E-02	0.16 vs. 0.10	**1.75E-06**

	uw/dm		WER	
Neanoconch vs. hatchling	0.05 vs. 0.04	**5.11E-04**	0.37 vs. 0.21	**9.74E-09**
Hatchling vs. submature	0.04 vs. 0.03	3.30E-02	0.21 vs. 0.15	**1.16E-04**
Neanoconch vs. submature	0.05 vs. 0.03	**8.82E-08**	0.37 vs. 0.15	**6.66E-15**

5. Standard deviations for specimens from siltstone (n = 63) and from shale (n = 40).

	ww/dm			ww/wh		
	Siltstone	Shale	p	Siltstone	Shale	p
Hatchling	0.05	0.05	3.62E-01	0.11	0.12	5.49E-02
Neanoconch	0.07	0.05	3.32E-02	0.17	0.13	3.69E-02
Submature	0.04	0.06	**2.93E-03**	0.07	0.12	**2.70E-05**

	uw/dm			WER		
Hatchling	0.04	0.04	1.58E-01	0.17	0.23	5.79E-02
Neanoconch	0.06	0.04	**7.02E-03**	0.37	0.30	8.90E-02
Submature	0.03	0.03	2.83E-01	0.11	0.15	1.83E-02

6. Standard deviations for specimens from multiple concretions (176; n = 12) and from a single concretion (176a; n = 16).

	ww/dm			ww/wh		
	176	176a	p	176	176a	p
Hatchling	0.02	0.03	1.80E-01	0.07	0.11	9.01E-02
Neanoconch	0.05	0.04	1.73E-01	0.13	0.10	1.70E-01
Submature	0.06	0.02	**4.21E-04**	0.08	0.03	**4.60E-04**

	uw/dm			WER		
Hatchling	0.02	0.03	1.49E-01	0.11	0.10	2.69E-01
Neanoconch	0.06	0.03	**9.22E-03**	0.36	0.16	**1.99E-03**
Submature	0.04	0.03	1.13E-01	0.13	0.05	**1.43E-04**

7. Coefficients of variation for all specimens (n = 103), siltstone (n = 63), shale (n = 40), locality 176 (n = 12), and concretion 176a (n = 16).

	ww/dm					ww/wh				
	All	Siltstone	Shale	176	176a	All	Siltstone	Shale	176	176a
Hatchling	7.62	7.51	7.76	3.70	5.33	8.45	7.49	9.08	4.88	8.28
Neanoconch	11.42	12.56	9.34	9.07	6.87	14.08	14.58	11.87	11.35	9.12
Submature	10.87	9.00	12.22	10.76	4.43	10.66	8.26	12.71	9.15	3.79
	uw/dm					WER				
Hatchling	17.65	15.52	18.28	8.35	11.71	9.05	7.48	9.78	5.37	4.40
Neanoconch	27.37	25.64	22.32	28.23	17.46	15.63	16.23	11.66	17.30	6.81
Submature	35.07	35.90	33.61	45.71	30.70	6.11	4.75	6.16	5.74	2.00

APPENDIX 2

Localities Listed in the Same Order as Table 1.

Locality information includes geographic description, stratigraphic assignment, year of collection, and names of collectors. Abbreviations: B = Yale Peabody Museum localities; D = U.S. Geological Survey localities; B176a and B192s = single concretions.

B185	Near Belle Fourche, SW¼ sec. 33, T. 10 N, R. 2 E, Butte County, South Dakota, Carlile Shale, 20 ft-thick (6.1 m) interval in Turner Sandy Member, 90.5 ft (27.6 m) above base, Landman and Waage, 1977
B186	Near Belle Fourche, NE¼ NW¼ sec. 10, T. 9 N, R. 2 E, Butte County, South Dakota. Carlile Shale, rusty weathering concretionary ledge 110.5 ft (33.6 m) above base of Turner Sandy Member, Landman and Waage, 1977
B187	Near Belle Fourche, center S½ sec. 29 and center N½ sec. 32, T. 10 N, R. 2 E, Butte County, South Dakota, Carlile Shale, concretionary interval 90.5-98.5 ft (27.6–30.0 m) above base of Turner Sandy Member, Landman and Waage, 1977
B198	Near Belle Fourche Reservoir, NE¼ SE¼ NE¼ sec. 18, T. 9 N, R. 4 E, Butte County, South Dakota, Carlile Shale, small red weathering concretions in Turner Sandy Member, Landman and Waage, 1977
B240	North of Shelby, sec. 3, T. 35 N, R. 2 W, Toole County, Montana, Marias River Shale, Ferdig Member, corresponds stratigraphically to bed no. 30 in middle unit of type section (Cobban et al., 1976), Landman and Kidwell, 1978
D9111	W½ sec. 3, T. 3 N, R. 85 W, Routt County, Colorado, Mancos Shale, Juana Lopez Member, from concretion 2 ft (0.6 m) below top of Juana Lopez Member
B176, B176a	SE¼ sec. 12, T. 36 N, R. 62 W, Niobrara County, Wyoming, Carlile Shale, septarian concretionary interval, about 30 ft (9.1 m) above base of Turner Sandy Member, "a" refers to individual concretion, Landman and Waage, 1977
B192, B192s	Near Edgemont, sec. 7, T. 9 S, R. 2 E, Fall River County, South Dakota, Carlile Shale, septarian concretionary interval, about 30 ft (9.1 m) above base of Turner Sandy Member, "s" refers to individual concretion, Landman and Waage, 1977
D7227	5 mi (8 km) east of Ferron, NW¼ sec. 9, T. 20 S, R. 8 E, Emery County, Utah, Mancos Shale, from a grey limestone concretion about 100 ft (30.4 m) above the base of the Ferron Sandstone Member, Gill and Cobban, 1969

All issues of *Novitates* and *Bulletin* are available on the web (http://digitallibrary.amnh.org/dspace). Order printed copies on the web from:
http://shop.amnh.org/a701/shop-by-category/books/scientific-publications.html

or via standard mail from:

American Museum of Natural History—Scientific Publications
Central Park West at 79th Street
New York, NY 10024

♾ This paper meets the requirements of ANSI/NISO Z39.48-1992 (permanence of paper).